Far-infrared absorption study of exciton ionization in germanium*

T. Timusk
Department of Physics, McMaster University, Hamilton, Ontario, Canada L8S 4M1
(Received 14 July 1975)

We use the strength of the far-infrared absorption of excitons at 3 meV as a measure of their concentration at a variety of temperatures and excitation densities. At low temperatures and densities the excitons are in equilibrium with electron-hole drops while in the region of 10°K they ionize to form an electron-hole plasma. A simple kinetic model shows that the location of the boundary on the phase diagram separating the high-temperature plasma from the exciton region depends on the electron-hole recombination rate. Different surface treatments appear to vary this rate, and in some cases a plasma density of 10^{15} cm^{-3} can be obtained. In the absence of a strong plasma, however, an exciton concentration of 5×10^{15} can be built up with no evidence of a lowering of exciton binding energy.

Excitons in germanium have traditionally been studied as a fine structure in the onset region of band-to-band transitions. In germanium, however, the exciton lifetime is very long (~7 μsec), and recently experiments have been reported[1] where a sufficient concentration of excitons have been generated to permit observation of the absorption arising from transitions between the ground state of excitons and their excited states. These transitions lie in the far infrared, and the experiments were carried out with a backward wave oscillator. In this paper we would like to use this absorption to study the temperature and density region where excitons can exist in germanium. We will show, using conventional far-infrared techniques, that excitons are in equilibrium with electron-hole drops at low temperatures and ionize to form a plasma at higher temperatures. The region where ionization occurs depends on the detailed kinetics of exciton recombination. We will also discuss briefly the problem of a metal-insulator transition in the exciton gas.

We use a crystal of pure germanium ($|N_d - N_a| \approx 8\times10^{10}$), 3.0×3.0×0.7 cm in size and polished with Syton to an optical finish. The crystal is immersed in helium exchange gas and the exciting *YAlG:Nd* laser is focussed to a spot of 0.5 mm diam on one of the large surfaces normal to a [111] principal axis of the crystal. The far-infrared probe radiation is confined to pass through the same area by a 1.2-mm-diam light cone.

Figure 1 shows the absorption spectrum of germanium at low temperatures with an excitation of 60 mW incident on the crystal. The spectrum at 4.9 °K is characterized by two strong lines at 3.0 and 3.5 meV and two weaker lines at 2.5 and 4.0 meV. There is a strong continuum extending from 4 meV to above 10 meV but very little absorption below 2.0 meV at low temperature. We associate this whole absorption with excitons. At higher temperatures the lines are markedly weaker, and a continuous spectrum appears below 2.0 meV. We suggest that this continuum arises from a plasma of electrons and holes in thermal equilibrium with the excitons. At temperatures below 4 °K the plasma absorption disappears, below 2 °K exciton peaks are weaker, and the strong electron-hole droplet resonance at[2] 8 meV can be

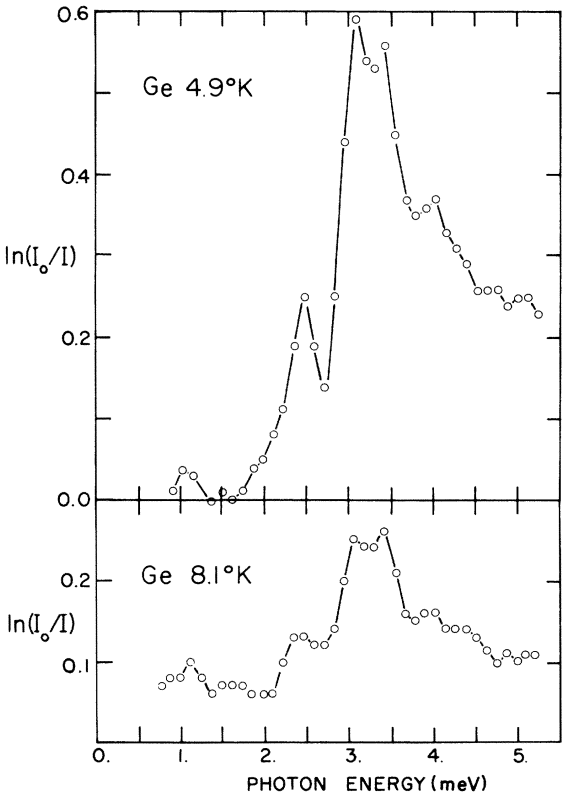

FIG. 1. Far-infrared absorption of germanium at two temperatures under 60-mW incident radiation. At the lower temperature only exciton absorption can be seen while at the higher temperature a plasma appears below 2 meV.

seen.

We can make use of the strength of the exciton absorption to estimate the exciton concentration. The well-known sum rule for the imaginary part of the dielectric constant ϵ'' is

$$\int_0^\infty \omega\epsilon''(\omega)\,d\omega = \tfrac{1}{2}\pi\omega_p^2 n^2$$

and the absorption constant $\kappa = \omega\epsilon''/cn$, where for germanium $n = 3.92$, the bulk value, and the plasma frequency of the excitons

$$\omega_p^2 = \frac{4\pi e^2}{n^2 m^*} n_{ex},$$

where n_{ex} is the exciton concentration and $m^* = 0.15$.[3] Taking the observed width of the exciton band as 5.0 meV and the diffusion length of the excitons 0.1 cm,[4] we obtain for the concentration

$$n_{ex} = 0.27 \ln(I_0/I) \times 10^{15}\ \text{cm}^{-3},$$

where I_0/I is the ratio of the incident to the transmitted radiation averaged over the region of the maximum of the exciton absorption from 3.0 to 3.5 meV. The exciton concentration can also be estimated from the absorbed laser power in a 1-mm-radius hemisphere with the assumption of unit quantum efficiency and a typical value for the exciton life time of[5] 7.7 μsec from the formula

$$n_{ex} = g\tau .$$

The second method gives a value higher by a factor of 3. The largest uncertainty in both methods is the diffusion length and spatial distribution of excitons. We have used a similar argument to estimate the plasma density using the continuous absorption which, because of its larger width, gives a lower numerical constant:

$$n_e = 0.47(\ln I_0/I) \times 10^{15}\ \text{cm}^{-3},$$

where the absorption is measured at 2.0 meV.

A further check on the calibration is the strength of the exciton absorption at the first appearance of the electron-hole drop absorption at 8 meV. Such threshold measurements have also been carried out on the drop luminescence in the near infrared.[6] Figure 2 shows the phase diagram for the electron-hole (EH) fluid that includes our threshold measurements and the work of Thomas *et al.*[6] on the liquid phase extrapolated to the low-density region past the critical point using a Guggenheim plot. The agreement here is reasonable. The solid line through our experimental points is a Richardson plot with an activation energy of 1.55 meV in agreement with luminescense measurements,[7] but it is known that actual binding energy of the fluid is higher due to lifetime and surface effects. We have found that it is possible to obtain exciton absorption strength in the far infrared that is higher than the points on the vapor pressure curve at higher excitation levels than those needed to just create drops. Presumably this is an effect of the expansion of the drops into the volume of the crystal subsequent evaporation of excitons.

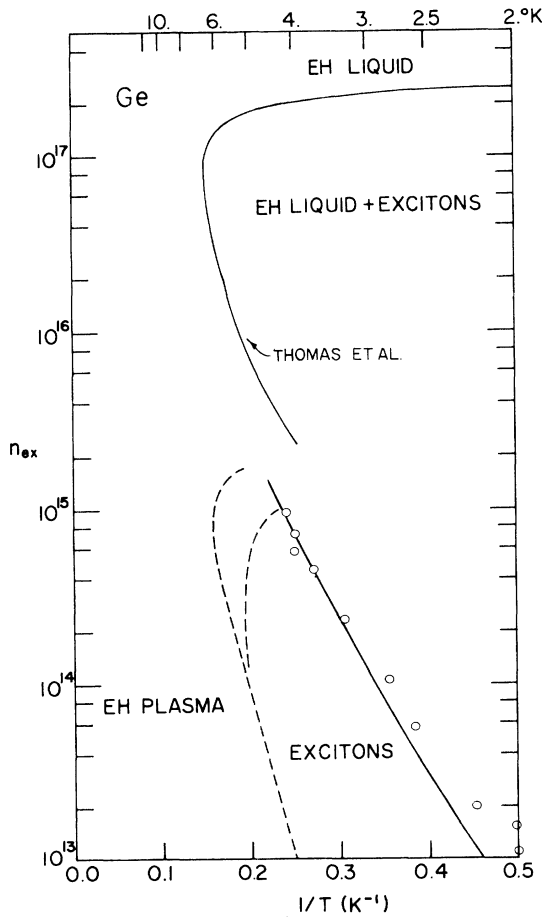

FIG. 2. Phase diagram of excitons in germanium. The phase boundary between the exciton gas and the region of EH liquid and gas was determined by these experiments (open circles) and fitted to a Richardson plot (solid line) with an activation energy for exciton of 1.55 meV. The dotted line denotes the region where the exciton concentration has dropped to half due to ionization. At higher densities the ionization curve is moved to lower temperatures by the reduction of exciton binding energy by the plasma. Two curves are shown at different electron lifetimes and recombination rates.

To study exciton ionization we use a simple kinetic model (Fig. 3). The rates of change of the exciton concentration $\dot{n}_{ex}$ and the free-electron concentration $\dot{n}_e$ are given by

$$\dot{n}_{ex} = (1/\tau_{ex})\, n_{ex} + \alpha n_e^2 - \beta n_{ex}$$

and

$$\dot{n}_e = g - \alpha n_e^2 + \beta n_{ex} - (1/\tau_e)\, n_e .$$

Here τ_{ex} and τ_e are the exciton and electron life-

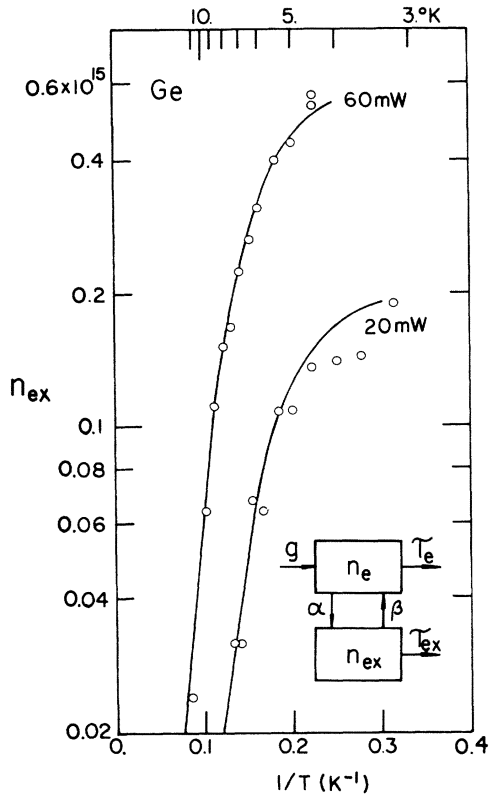

FIG. 3. Exciton concentration as a function of temperature at different excitation levels. At higher temperatures the dependence on excitation approaches quadratic. The solid curves are the results of a kinetic model shown schematically in the insert.

times and g the generation rate of electrons and holes. The rate of recombination α of excitons we assume to be a temperature-independent constant and exciton ionization rate β we take to be[7]

$$\beta = (2\pi kT/\hbar g_{ex}) e^{-E_{ex}/kT},$$

where $g_{ex}=2$ is the ground-state degeneracy of the exciton and E_{ex} the exciton ionization potential. The hole concentration in our intrinsic sample will be equal to the electron concentration. Setting the time derivatives equal to zero we can solve for n_{ex}:

$$n_{ex}=\frac{(\beta\tau_{ex}+1)}{2c}\left[1-\left(1+\frac{4c}{(\beta\tau_{ex}+1)}g\tau_{ex}\right)^{1/2}\right]+g\tau_{ex}, \tag{1}$$

where $c=\alpha\tau_{ex}(\tau_e/\tau_{ex})^2$. Two limiting cases are of interest:

$$n_{ex}=g\tau_{ex}, \qquad kT\ll E_{ex}, \quad cg\tau_{ex}\gg 1,$$

$$n_{ex}=(\alpha/\beta)(g\tau_e)^2, \quad kT\approx E_{ex}.$$

Thus, as the temperature increases, the exciton concentration changes from a linear to a quadratic function of the excitation rate.

Figure 3 shows the exciton concentration as a function of temperature at two levels of excitation. The solid lines are fits to Eq. (1) with the following set of parameters:

$$g=0.75\times10^{21}\ \text{cm}^{-3}\ \text{sec}^{-1},\quad \tau_e=5\times10^{-7}\ \text{sec},$$

$$\tau_{ex}=10^{-6}\ \text{sec},\quad c=1.2\times10^{-11}\ \text{cm}^3\ \text{sec}^{-1},$$

$$E_{ex}=3.6\pm0.3\ \text{meV}.$$

It will be seen that the two curves are described adequately by the same set of parameters and the ionization energy is in reasonable agreement with spectroscopic values.[8] We have used the Drude theory and the shape and strength of the plasma absorption to estimate the electron concentration and find an electron lifetime τ_e of 5×10^{-7} and a collision time of 6×10^{-14} for this particular sample.

One might expect the kinetic model to fail at the highest densities reached in these experiments. The density of excitons is approaching the criterion for an insulator-metal transition (Thomas *et al.*, Ref. 6):

$$n_{MI}=(1/8\pi)(kT/E_{ex})a_0^{-3}$$

$$=1.6\times10^{15},$$

with $T=5$ °K, $E_{ex}=4.1$ meV, and $a_0=110$ Å.[8] (This last figure is an estimate based on a 4.1-meV binding energy.) This transition may manifest itself in a number of ways; one might see a shift and broadening of the exciton lines or the appearance of a plasma absorption at temperatures below those expected from the rate equations.

To describe this effect we can use a Debye screening model for the lowering of ionization potential used in conventional ionized-gas theory.[9] From this point of view the electron-hole density lowers the ionization potential from E_0 the low density value to

$$E_{ex}=E_0-(e^2/\epsilon)(8\pi e^2 n_e/\epsilon kT)^{1/2}.$$

This effect causes the ionization boundary on the phase diagram to shift to lower temperatures in the density region $\sim10^{15}$ cm^{-3}. The effect depends critically on the electron-hole density and therefore on the parameters α and τ_e in our kinetic model. We have shown two such calculated curves on the phase diagram (Fig. 2) corresponding to electron lifetimes that differ by a factor of 3. We have not done a detailed test of this model.

Up to a density 5×10^{15} cm^{-1} we have observed no shift or broadening of the exciton absorption at 4 °K. While a small amount of broadening in particular is difficult to observe in the presence of nonuniform density we can place 0.1 meV as the limits on the shift and 0.1 meV on the width.

The strength of the plasma we find is strongly dependent on the surface treatment. The strongest

plasma, $n_e = 10^{15}$ cm^{-3}, is seen in crystals that have been etched and polished with Syton, while crystals that have been mechanically polished and subsequently Syton polished and not etched show a very weak plasma.

I would like to acknowledge the experimental assistance of M. A. Buchanan and A. Silin, valuable suggestions by T. M. Rice and J. M. Worlock, and discussion with G. A. Thomas, J. C. Hensel, and M. Combescot.

---

*Work supported in part by the National Research Council of Canada.

[1]E. M. Gershenzon, G. N. Golt'sman, and N. G. Ptitsyna, Zh. Eksp. Teor. Fiz. Pis'ma Red. 16, 228 (1972) [Sov. Phys. JETP-Lett. 16, 161 (1972)]; Mandel'shtam and V. N. Murzin, *ibid.* 17, 480 (1973) [*ibid.* 16, 345 (1973)].

[2]V. S. Vavilov, V. A. Zayats, and V. N. Murzin, Zh. Eksp. Teor. Fiz. Pis'ma Red. 10, 304 (1969) Sov. Phys. JETP-Lett. 10, 195 (1969) .

[3]This value of the effective mass was obtained by fitting the sum rule to the donor and acceptor results of J. H. Reuszer and P. Fisher, [Phys. Rev. 135, A 1125 (1964)] and R. J. Jones and P. Fisher, [J. Phys. Chem. Solids 26, 1125 (1965)]. It is higher than the optical mass of 0.046 of W. F. Brinkman and T. M. Rice, [Phys. Rev. B 7, 1508 (1973)]. Because of these uncertainties we have adopted the absorbed laser power calibration in all our diagrams.

[4]Ya. E. Pokrovskii and K. I. Svistunova, Fiz. Tverd. Tela 13, 1485 (1971) [Sov. Phys.-Solid State 13, 1241 (1971)]; R. W. Martin, Phys. Status Solidi B 61, 223 (1974).

[5]B. M. Westervelt, T. K. Lo, J. L. Staeli, and C. D. Jeffries, Phys. Rev. Lett. 32, 1051 (1974).

[6]Y. A. Pokrovskii, Phys. Status Solidi A 11, 385 (1972); Thomas K. Lo, Bernard J. Feldman, and C. D. Jeffries, Phys. Rev. Lett. 31, 224 (1973); G. A. Thomas, T. G. Phillips, T. M. Rice, and J. C. Hensel, *ibid.* 31, 3861 (1973); and G. A. Thomas (private communication).

[7]K. J. Laidler, *Theories of Chemical Reaction Rates* (McGraw-Hill, New York, 1969), p. 41.

[8]V. I. Sidorov and Ya. E. Pokrovskii, Fiz. Tekh. Poluprovodn. 6, 2405 (1972) [Sov. Phys.-Semicond. 6, 2015 (1973)].

[9]Donald G. Clayton, *Principles of Stellar Evolution and Nucleosynthesis* (McGraw-Hill, New York, 1968), p. 139.